LARGE-SCALE BIOLOGY ARTICLE

Differentially Phased Leaf Growth and Movements in *Arabidopsis* Depend on Coordinated Circadian and Light Regulation[W]

Tino Dornbusch,[a] Olivier Michaud,[a] Ioannis Xenarios,[b] and Christian Fankhauser[a,1]

[a] Center for Integrative Genomics, Faculty of Biology and Medicine, University of Lausanne, 1015 Lausanne, Switzerland
[b] SIB-Swiss Institute of Bioinformatics, University of Lausanne, 1015 Lausanne, Switzerland

In contrast to vastly studied hypocotyl growth, little is known about diel regulation of leaf growth and its coordination with movements such as changes in leaf elevation angle (hyponasty). We developed a 3D live-leaf growth analysis system enabling simultaneous monitoring of growth and movements. Leaf growth is maximal several hours after dawn, requires light, and is regulated by daylength, suggesting coupling between growth and metabolism. We identify both blade and petiole positioning as important components of leaf movements in *Arabidopsis thaliana* and reveal a temporal delay between growth and movements. In hypocotyls, the combination of circadian expression of *PHYTOCHROME INTERACTING FACTOR4* (*PIF4*) and *PIF5* and their light-regulated protein stability drives rhythmic hypocotyl elongation with peak growth at dawn. We find that PIF4 and PIF5 are not essential to sustain rhythmic leaf growth but influence their amplitude. Furthermore, EARLY FLOWERING3, a member of the evening complex (EC), is required to maintain the correct phase between growth and movement. Our study shows that the mechanisms underlying rhythmic hypocotyl and leaf growth differ. Moreover, we reveal the temporal relationship between leaf elongation and movements and demonstrate the importance of the EC for the coordination of these phenotypic traits.

INTRODUCTION

The survival of most organisms on Earth depends on plants using solar energy, water, nutrients, and CO_2 to fuel their own growth. The conversion of solar into chemical energy happens primarily in leaves, but surprisingly little is known about the regulation of the growth of leaves themselves. It has been shown that growth of leaves and other plant structures occurs with a diel (24-h) rhythm (Nozue et al., 2007; Wiese et al., 2007; Yazdanbakhsh et al., 2011; Farré, 2012; Ruts et al., 2012a), which is not entirely surprising given that the ever-occurring day-night alternations profoundly affect plant metabolic reactions. The circadian clock and leaf starch metabolism regulate the growth patterns of roots and leaves (Wiese et al., 2007; Yazdanbakhsh et al., 2011; Ruts et al., 2012b). However, detailed kinetics of diel leaf growth rhythms, a prerequisite to understand the molecular mechanisms underlying growth control, remain scarce (Wiese et al., 2007; Ruts et al., 2012b). This presumably results from leaf movements accompanying leaf growth, thereby complicating growth analysis in living plants (Wiese et al., 2007).

Growth rhythms are best understood in hypocotyls (one-dimensional) where they depend on coordinated regulation by light, the availability of carbon, and the circadian clock (Nozue et al.,

2007; Nusinow et al., 2011; Stewart et al., 2011). In the presence of sufficient resources, rhythmic hypocotyl growth peaks at the dark-light transition (dawn). This rhythm depends on an external coincidence mechanism whereby circadian expression of *PHYTOCHROME INTERACTING FACTOR4* and *5* (*PIF4* and *PIF5*) and light-regulated degradation of these basic helix-loop-helix factors leads to their maximal activity around dawn (Nozue et al., 2007). Repression of *PIF4* and *PIF5* expression earlier in the night depends on the evening complex, which is composed of EARLY FLOWERING3 (ELF3) and ELF4 and LUX ARRHYTHMO, and prevents excessive growth earlier in the night (Nusinow et al., 2011).

Different types of movements accompany rhythmic leaf growth (Wiese et al., 2007; Whippo and Hangarter, 2009; Dornbusch et al., 2012). Diel leaf movements are a well-characterized output of the circadian clock (Farré, 2012). In addition, movements with much shorter periods known as circumnutations occur in many plant structures including growing leaves (Stolarz, 2009; Whippo and Hangarter, 2009). All these movements are known to be associated with growth and/or reversible cell enlargement at the level of the petiole (the structure connecting the leaf blade to the stem). In some plant species, such as *Mimosa pudica*, specialized cells at the base of the petiole form the pulvinus that allows for rapid reversible changes in leaf position (Whippo and Hangarter, 2009). Plants like *Arabidopsis thaliana*, which do not possess such pulvini, also undergo leaf movements that at least partially depend on differential growth of the adaxial and abaxial sides of the petiole (Polko et al., 2012; Rauf et al., 2013). However, the coordination and relationship between leaf movements and growth remain largely unknown.

The movements accompanying rhythmic leaf growth render kinetic growth analyses challenging, prompting some authors to prevent leaf movements to measure growth (Wiese et al., 2007). Moreover, simultaneous analyses of leaf growth and movements have not been reported previously, thereby making it difficult to understand the relationship between these phenomena. Here, we used near-infrared laser scanning and developed imaging algorithms that allow us to follow growth, nutations, and movements of the same leaves with high spatial and temporal resolution. We found that leaves accelerate elongation growth several hours prior to upward movements of the leaves (leaf hyponasty). Proper phasing between elongation and hyponasty depends on ELF3, a member of the evening complex. As in hypocotyls, leaf growth rhythms in day-night conditions are coordinately regulated by the interplay between light and circadian signals. However, our results in leaves show that the underlying molecular mechanism differs from the one that was previously uncovered for the regulation of hypocotyl growth.

RESULTS

Development of a Method for Simultaneous Analysis of Leaf Growth and Movements

To analyze the relationship between leaf growth and leaf movements, we developed an image analysis algorithm to measure single leaves using a previously described laser scanning method (Dornbusch et al., 2012). *Arabidopsis* plants were imaged at intervals of 60 min and time-lapse images were analyzed to track points at the base (P_0), petiole-blade-junction (P_P), and the tip (P_T) of each individual leaf (Figure 1A; Supplemental Figure 1 and Supplemental Movie 1). The vector P_0P_T defines length l_{tip} and elevation angle Φ_{tip} of each leaf, while the analogous traits for the petiole vector and blade vector are l_{pet}, Φ_{pet} and l_{bl}, Φ_{bl}, respectively (Figure 1A). A more detailed geometric definition of these traits is given in the Supplemental Methods. The leaf-tracking algorithm was validated comparing data from the laser scanning system with measurements on simultaneously photographed plants (Figures 2A and 2B; Supplemental Movie 2). This analysis demonstrated the precision of our system (Figures 2C and 2D). Although l_{tip} is somewhat shorter than the precise leaf length (l_{leaf}; Figure 1A), we showed that diel leaf elongation rate (integrated over 24 h) and the growth rhythms were highly similar for both l_{tip} and l_{leaf} (Figure 1B). Therefore, in the following, we primarily used the leaf elongation rate computed from l_{tip} to discuss the diurnal pattern of growth. Note that leaf expansion in width is not captured here and may occur at different times or rates. For simplicity, we refer to elongation rates as growth and changes in elevation angles as movements (Supplemental Figures 2A and 2B). When imaged at 10-min intervals, we can also measure ultradian circumnutations (nutations) that are distinct from the diurnal leaf movements (Supplemental Figure 2C).

Due to geometric constraints from the measuring device, the entire leaf can be scanned with the most precision in plants with relatively horizontal leaves. This dictated our choice to start our analysis with plants grown in long days (L/D, 16/8 h) that were released into continuous days (L/L) where the leaf positions remain relatively horizontal. Both growth and movements followed a rhythmically oscillating pattern consistent with circadian regulation of growth and movement (Figure 3; Supplemental Figure 2). By simultaneously analyzing growth rates and movements, we observed that the phase of both peaks was distinct (Figure 3; Supplemental Figure 2). Growth was minimal during the subjective night around zeitgeber time 20 (ZT20) and peaked in the subjective morning around ZT3-4. Leaf elevation angle Φ_{tip}
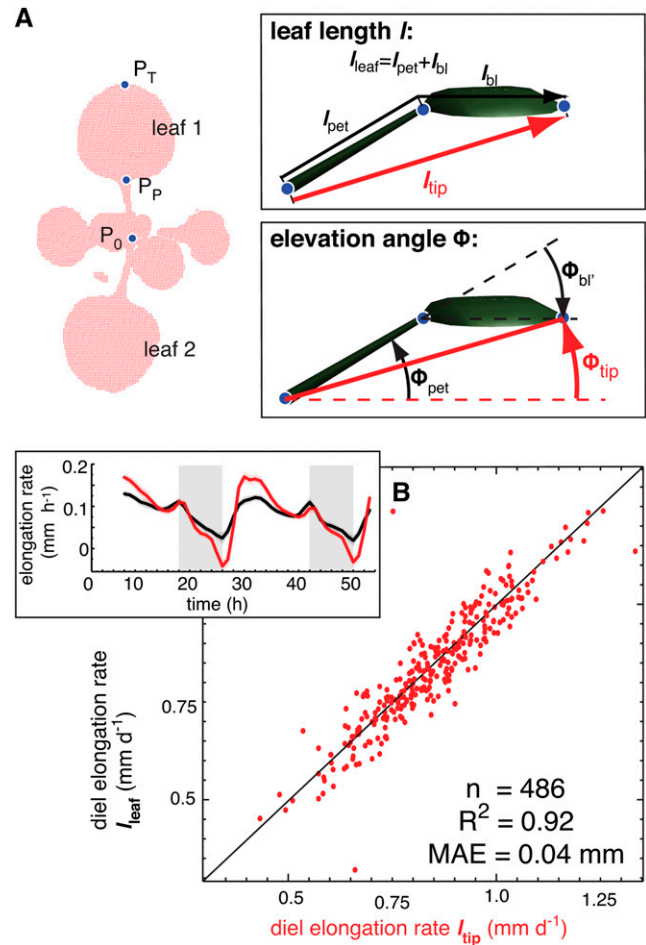
Figure 1. Definition of Measured Traits.

(A) Geometric definition of leaf length and elevation angle. *Arabidopsis* plant as a measured 3D point cloud (red dots) viewed from top down. The points P_0 (position of meristem), P_P (position of petiole-blade junction), and P_T (position of leaf tip) define length (l) and elevation angle (Φ) of the whole leaf (l_{tip}, Φ_{tip}), of the petiole (l_{pet}, Φ_{pet}), and of the blade (l_{bl}, Φ_{bl}) as illustrated in the insets.

(B) Comparison of diel (24 h) elongation rate using l_{tip} and elongation rate using l_{leaf} of leaf 1 and 2. One data point reflects one measurement per leaf per day. n = number of data points, R^2 = coefficient of determination, MAE = mean absolute error. Col-0 plants were grown for 14 d in long-day conditions (L/D, 16/8) before measurement in L/D; the inset shows time courses of elongation rate as moving average over 3 h using l_{leaf} (black line) or using l_{tip} (red line); vertical gray bars represent true night periods. The colored opaque band (same color as mean line) is the 95% confidence interval of mean estimate (solid line).
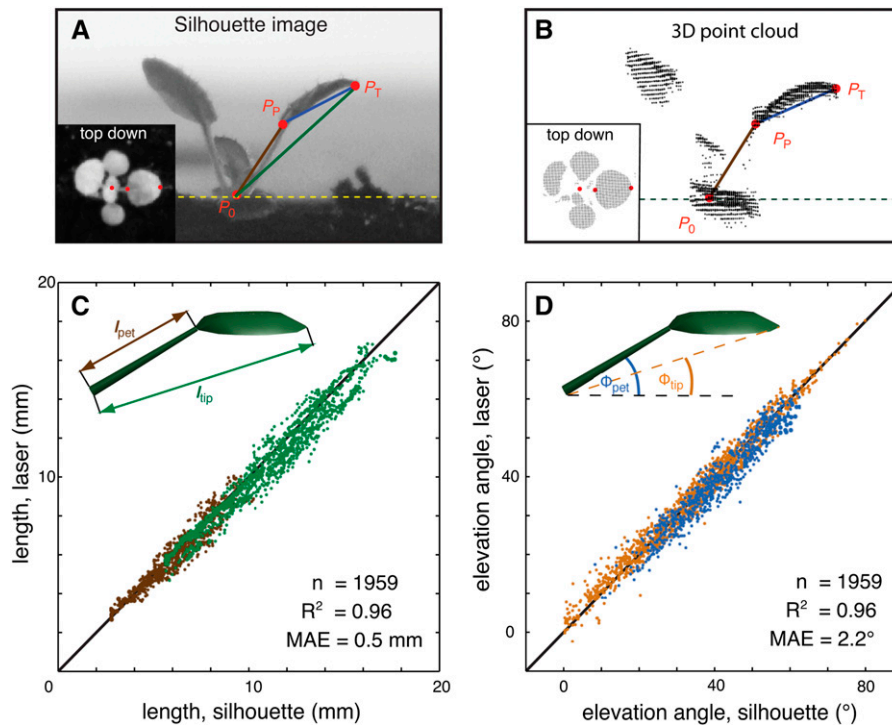
Figure 2. Development and Validation of a Method for Live Measurements of Leaf Growth and Leaf Movements.

(A) Silhouette image taken with an infrared-sensitive camera from the side and top-down (inset); three characteristic points define the dimension and orientation of each leaf and were manually selected: P_0, shoot apical meristem; P_P, blade-petiole junction; P_T, leaf tip.
(B) The laser scanner renders the plant surface as a 3D point cloud. The points P_0, P_P, and P_T are computed for each leaf using a semiautomated image analysis algorithm. We simultaneously photographed and scanned 27 individual leaves over 48 h and compared values for P_0, P_P, and P_T determined with each method.
(C) Length of petiole (brown dots) and leaf (green dots) measured from silhouette images (x axis) plotted against corresponding values computed with our algorithm (y axis).
**(D)** Petiole elevation angle (blue dots) and leaf elevation angle (orange dots) measured from silhouette images (x axis) plotted against corresponding values computed with our algorithm (y axis). One data point reflects one measurement per leaf per time step. Data of five different repeated control experiments were grouped together. Solid black line is the 1:1 line, n = number of data points, R^2 = coefficient of determination, and MAE = mean absolute error.

was minimal around ZT2 and reached a maximum in the subjective evening at ZT14 (Figure 3C; Supplemental Figure 2B). To better compare the growth rate with movement, we also plotted the rate of change of leaf position (in °h^{-1}) (Figures 3D and 4A). This method allows comparing acceleration of growth (slope in Figure 3B) with acceleration of up- and downward movement (slope in Figure 3D). It confirms a phase difference of ~3 h between acceleration of growth and movement (Figure 4A). Finally, we noticed that upward movement of leaves largely coincided with a phase of nutations that faded out around ZT16, when leaves started to move down (Supplemental Figure 2C).

Both Petiole and Blade Contribute to the Patterns of Leaf Growth and Hyponasty

By analyzing leaf growth and movement, we identified the temporal relationship between the phases of upward movement and acceleration of growth (Figures 3 and 4A). To uncover how blade and petiole contribute to these patterns, we measured them

separately. Our measurements revealed that at ZT20 the leaf blade started to elongate several hours before the petiole (Figure 4B, arrows). This initial blade growth phase occurred at a time when both the petiole and the blade still moved down, explaining why the leaf tip moved downwards around subjective dawn (Figure 3C). The leaf blade accelerated its movement around ZT0 (Figure 4C) and moved upwards when it reached its maximal elongation rate (approximately ZT2), a time that also corresponded to an increase in petiole growth rate (Figure 4B). Petioles moved with similar amplitude as blades and accelerated their movement shortly after blades, but at a slower rate (Figure 4C). Similarly to the blades, they started to move upwards when reaching their maximal growth rate (Figures 4B to 4D). Finally, we noticed that while blade growth showed one growth peak shortly after subjective dawn, the petiole showed a morning growth peak and a second one before subjective dusk (Figure 4B). Petiole growth around ZT12 may explain the second growth peak observed in L/L conditions (Figures 3B and 4B). These experiments indicate that around subjective dawn both growth and movement first start in the blade and then in the
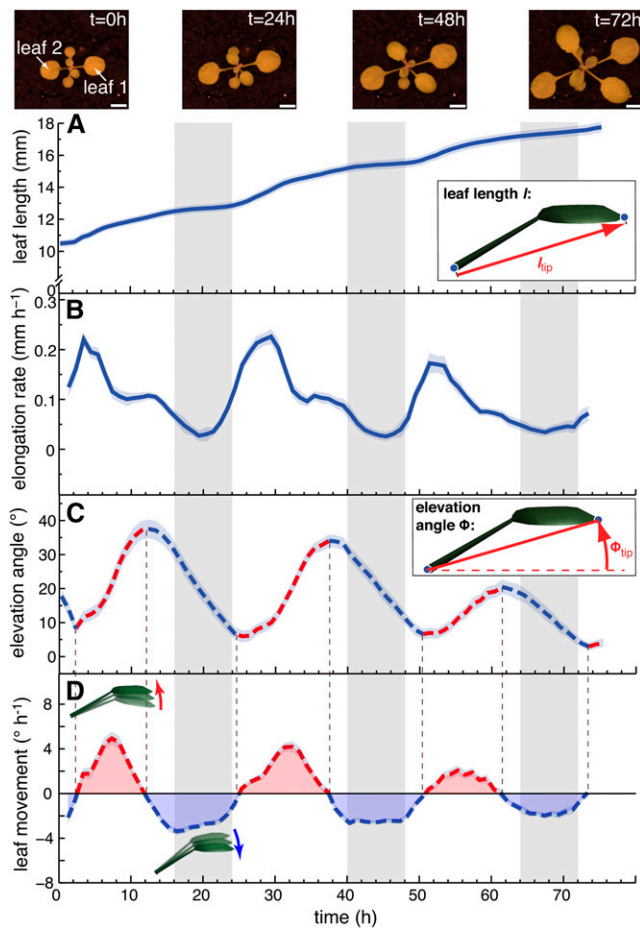
Figure 3. The Pattern of Leaf Growth and Movements in Constant Light.

Length **(A)**, elongation rate **(B)**, elevation angle **(C)**, and movements **(D)** (angular rate of change) of leaves 1 and 2 in continuous day (L/L) measured on 43 leaves (30 plants). l_{tip} (**[A]** and **[B]**) and Φ_{tip} (**[C]** and **[D]**) were used to compute the graphs. Images on top show a representative plant at times (t = 0, 24, 48, and 72 h) during the experiment (bar = 5 mm). Parts of the graph in **(C)** highlighted in red represent phases of upward and parts highlighted in blue phases of downward movement. Col-0 plants were grown for 14 d in standard L/D conditions. At time 0 h (ZT0), lights were switched on for imaging and kept on in L/L. Vertical gray bars represent subjective night periods. Leaf elongation rate was computed as mean moving average (3 h) of 43 individual curves. Leaf elevation angle and movement rates are mean values. The opaque band around the mean lines is the 95% confidence interval of mean estimate.

petiole. Moreover, in both parts of the leaf rapid upward movement starts significantly later than acceleration of growth (Figures 3 and 4).

To determine whether leaf blade position also contributes to leaf hyponasty in other growth conditions, we analyzed blade and petiole position in L/D-grown plants and in plants transferred into simulated shade, which is known to enhance leaf hyponasty (Moreno et al., 2009; Dornbusch et al., 2012). In both conditions, blade movement clearly contributed to overall leaf hyponasty (Supplemental Figures 3 and 4). Moreover, both in L/D conditions and in response to simulated shade, the blade started to move upwards prior to the petiole (Supplemental Figures 3 and 4, arrows).

Collectively, these experiments identify the movement of the blade as an important contributor to leaf hyponasty and show that blade movement precedes petiole movements.

Changes in the Light Environment Differentially Affect Leaf Growth and Movements

Earlier studies in *Arabidopsis* have identified a differential growth response between the adaxial and abaxial sides of the petiole as a mechanism underlying leaf hyponasty (Polko et al., 2012; Rauf
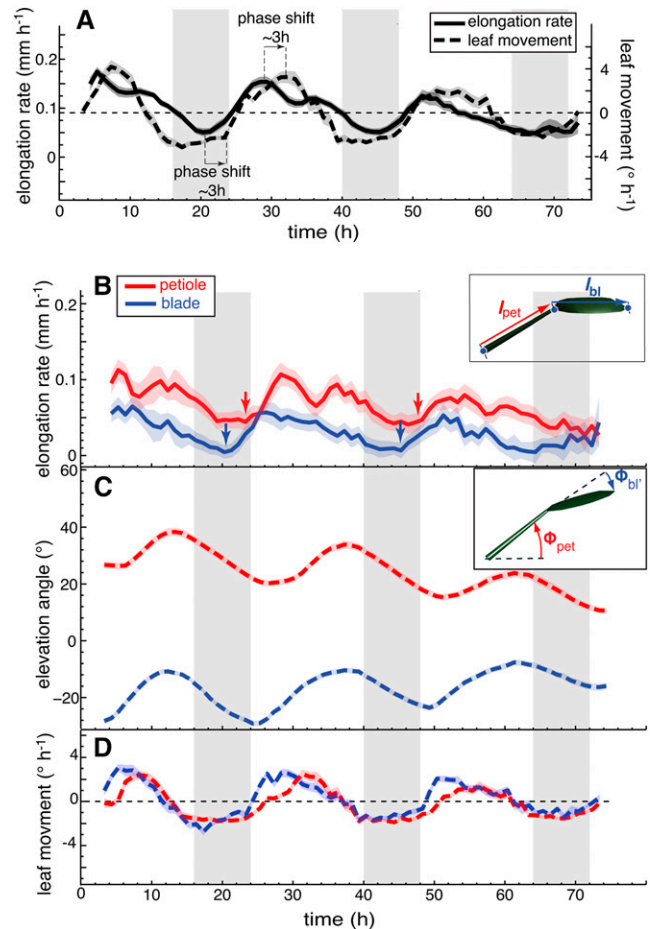
Figure 4. Blade and Petiole Movements Contribute to the Leaf Hyponastic Response.

(A) Leaf elongation rate and leaf movements (angular rate of change) of leaves 1 and 2 in continuous day were replotted from Figures 3B and 3D for better direct comparison.
**(B)** to **(D)** Leaf elongation rate **(B)**, leaf elevation angle **(C)**, and leaf movements **(D)** (angular rate of change) of petioles (in red) and blades (in blue) of leaves 1 and 2 in continuous day (L/L) measured on 32 leaves. Col-0 plants were grown for 14 d in standard L/D conditions. At time 0 h, lights were switched on for imaging and kept on in L/L. Vertical gray bars represent subjective night periods. Leaf elongation rate is computed as mean moving average (3 h) of 32 individual curves. Leaf elevation angle and movement rates are mean values. The opaque band around the mean lines is the 95% confidence interval of mean estimate. Arrows indicate acceleration of growth.

et al., 2013). This suggests that *Arabidopsis* leaf hyponasty is primarily a growth-driven process. Our work shows that there is a temporal shift between growth and movement (Figures 3 and 4; Supplemental Figures 3 and 4), suggesting a more complex relationship between these two processes. To test this further, we analyzed growth and movement in plants grown in different light regimes and plotted diel (24 h) growth rates and diel leaf movements (Figure 5). This comparison showed that a decrease in PAR and a decrease in daylength alter the relationship between growth and movements. In short-day conditions (S/D), diel leaf growth rate was decreased, whereas the magnitude of diel movements was similar in S/D compared with L/L or L/D (Figure 5). Low PAR-grown plants also showed decreased growth but increased diel leaf movements compared with L/L or L/D (Figure 5) consistent with other findings of low-PAR-induced hyponasty (Keller et al., 2011). These experiments suggest a partial uncoupling between the magnitude of growth and movement.

Light Is Required to Initiate Leaf Growth at Dawn

Rhythmic growth of hypocotyls is regulated by a combination of circadian and light cues (Nozue et al., 2007); we thus compared leaf growth and movements between plants maintained in day-night
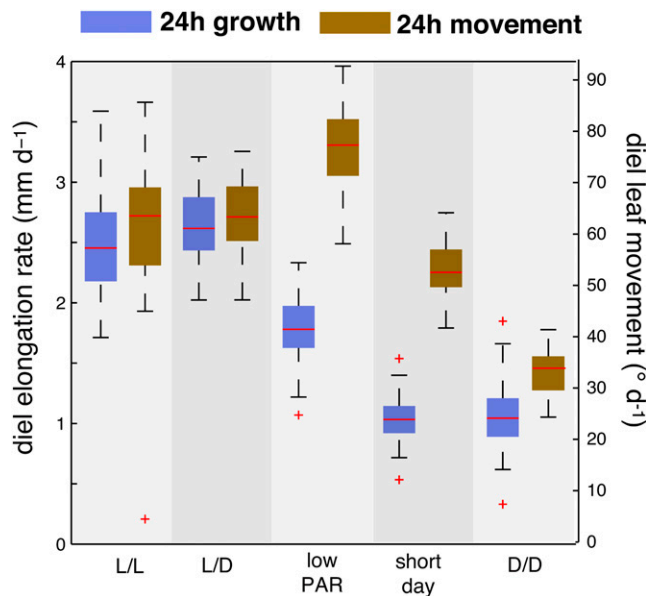

Figure 5. The Magnitude of Growth and Movements Is Differentially Affected by Decreasing Light Intensity and Daylength.

Diel leaf elongation rate and leaf movement of leaves 1 and 2 (24 h period). Diel elongation rates and leaf movements (absolute changes in leaf elevation angle) were computed by summing hourly rates over a period of 24 h starting from ZT2.25. Col-0 plants were grown for 14 d in standard L/D conditions (16/8 h). At time 0 h, plants were imaged for 24 h in constant light (L/L; n_{leaf} = 43), maintaining day-night cycles (L/D, n_{leaf} = 27), reducing the light intensity (low PAR) but maintaining L/D (PAR=35 µmol m^{-2} s^{-1}; n_{leaf} = 57) and in continuous darkness (D/D; n_{leaf} = 41). For the S/D experiment Col-0 was grown for 18 d in S/D (8/16 h) before imaging under the same conditions (n_{leaf} = 47). n_{leaf} = number of measured leaves.

and plants released into constant light (L/L). In L/L, growth rates started to rise several hours before the subjective dawn (ZT20), whereas in L/D, growth did not recover until dawn (ZT0). As light was given, the growth rate rose very quickly to reach the same rate as in LL (Figure 6A, arrows). In L/D-grown plants, the increase of the growth rate coincided with lights on but the timing of the morning peak was similar in L/D and L/L (Figure 6A). The second growth peak preceding dusk at ZT16 was more pronounced in L/D than L/L (Figure 6A). The diurnal pattern of the leaf elevation angle was similar in L/D and L/L. Minimum values for Φ_{tip} were observed at the time of the morning growth peak at ZT3 and maximum values around ZT13-14 (Figure 6B). Hence, similar phasing between growth and movements was maintained in both conditions (Figure 6B). In our growth chamber, light-dark transitions are abrupt. At dusk, this coincided with a transient upward movement (strong acceleration of movement) (Figures 6B and 6C). Downward movement accelerates in the second half of the night followed by a brief reacceleration of first downward then upwards movement at dawn (Figure 6C). Our data thus show that the circadian clock regulates both movement and growth rhythms and that day-night transitions influence these patterns.

When grown in day-night conditions, the leaf growth rate was at its minimum at the end of the night (ZT0) and rapidly increased after dawn (Figure 6). To test whether light is essential to induce growth in the morning, we entrained plants in L/D (16/8 h) and imaged them prolonging the night for 3 h before dusk (L/$_{+3}$D) or after dawn (L/D$_{+3}$). At L/D$_{+3}$, leaves did not start growing at ZT0 but at actual dawn ZT3 (Figure 7A; Supplemental Figure 5A). At L/$_{+3}$D, the first growth peak remained at ZT0, but the second growth peak was shifted to ZT13 (Figure 7B; Supplemental Figure 5B). To determine whether light is sufficient to trigger growth, we shortened the night by 3 h (L/$_{-3}$D). Early onset of the day (L/$_{-3}$D) triggered growth, although not as sharply as dawn in plants grown in L/D (Figure 7C; Supplemental Figure 5C). These experiments show that light at dawn has a profoundly different effect on growth of hypocotyls and leaves: In leaves it triggers growth (Figures 6 and 7), while in hypocotyls it inhibits it (Nozue et al., 2007).

The need for light at dawn to initiate leaf growth could result from the need for photosynthates. We decided to indirectly test this idea by growing plants in different light regimes. Plants partition more resources into starch when grown in short days (S/D) than in long days, suggesting that they may have more resources available to fuel growth early in the morning when grown in L/D (Stitt and Zeeman, 2012; Sulpice et al., 2014). We therefore compared growth and movements in S/D- and L/D-grown plants and found that in both conditions, growth in the morning required light and that the morning growth peak was reduced in S/D compared with L/D (Supplemental Figure 6A). In contrast to L/D conditions, we could not detect a second growth peak preceding dusk (ZT8), but rather a peak during the night at ZT12 (Supplemental Figure 6A). Overall growth was reduced in S/D-grown plants but more growth (in relative terms) occurred at night in S/D-grown plants than in L/D plants (Supplemental Figure 6A). As S/D-grown plants invest more resources into starch, this finding is compatible with a metabolic role of light in the regulation of growth patterns (Stitt and Zeeman, 2012; Sulpice et al., 2014). In contrast to diel growth rates, daylength moderately affected the pattern and the magnitude of diel leaf movements, except that dusk
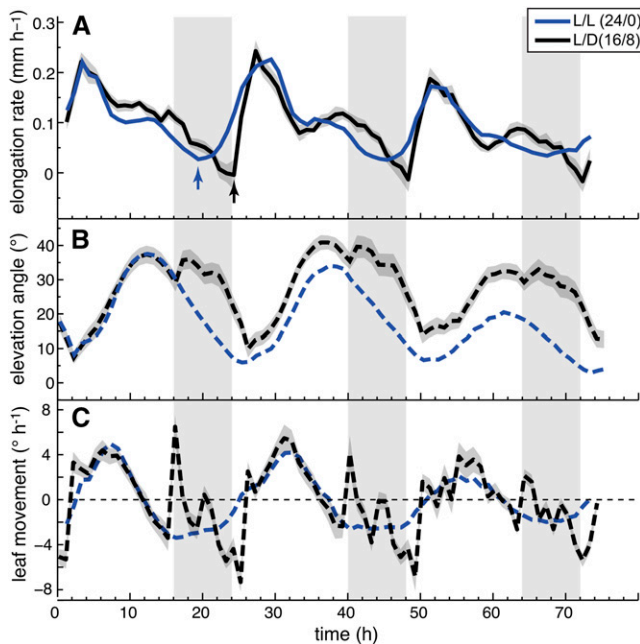
Figure 6. Day-Night Transitions Alter Rhythmic Growth and Movements.

Leaf elongation rate **(A)**, leaf elevation angle **(B)**, and leaf movements **(C)** (angular rate of change) of leaves 1 and 2 in continuous day (L/L; blue line; n_{leaf} = 43) and long-day conditions (L/D; 16/8; black line, n_{leaf} = 27). Col-0 plants were grown for 14 d in standard L/D conditions. Beginning from time 0 h, plants were imaged either in L/L or in L/D. Vertical gray bars represent subjective or true night periods. Leaf elongation rate was computed as mean moving average (3 h) of individual curves. Leaf elevation angle and movement rates are mean values. The opaque band around the mean lines is the 95% confidence interval of mean estimate. Arrows indicate acceleration of growth and n_{leaf} = number of measured leaves. l_{tip} and Φ_{tip} were used to compute the graphs.

altered leaf position in L/D but not in S/D (Figure 5; Supplemental Figure 6A).

Our results suggest that light-induced metabolism is required to promote leaf growth. To test this further, we compared growth of L/D-grown plants in either in high or low PAR and found that in low PAR the magnitude of leaf growth was reduced (Figure 5). We also transferred L/D-grown plants into D/D, which led to a decrease in the diel growth rate (Figure 5). Consistent with our night extension experiment (Figure 7A), there was no growth induction shortly after subjective dawn in D/D (Supplemental Figure 6B); however, there was a transient growth peak around ZT6-8 (Supplemental Figure 6B). Upon return into the light, the leaf growth rate increased rapidly (Supplemental Figure 6B, black arrow). Taken together, our results are consistent with a metabolic role of light to initiate leaf growth at dawn (Figures 5 to 7; Supplemental Figures 5 and 6).

The Phase Relationship between Leaf Growth and Movements Requires a Functional Evening Complex

Our results show that day-night cycles interplaying with the circadian clock orchestrate the diurnal patterns of growth and movement. Rhythmic hypocotyl growth is also coordinately controlled by the circadian clock and light cues that converge

on the regulation of PIF4 and PIF5 (Nozue et al., 2007). We thus analyzed leaf growth and movements of *pif4 pif5* double mutants and found that, when grown in long days, this mutant displayed low amplitude growth and movement rhythms that were otherwise similar to those of the wild type (Figure 8A). Overexpression of PIF4 or PIF5 and photoreceptor mutants caused a reduction of the amplitude in hypocotyl growth rhythms (Nozue et al., 2007). The situation was different for leaf growth as PIF4 overexpression and *phyB* mutants maintained robust leaf growth rhythms, although in these mutant backgrounds, there was more leaf growth toward the end of the day (Supplemental Figure 7). High PIF4 and PIF5 activity is prevented early in the night by the evening complex that restricts the expression of *PIF4* and *PIF5* and hypocotyl growth during the night (Nozue et al., 2007; Nusinow et al., 2011). To investigate the role of the evening complex in rhythmic leaf growth,
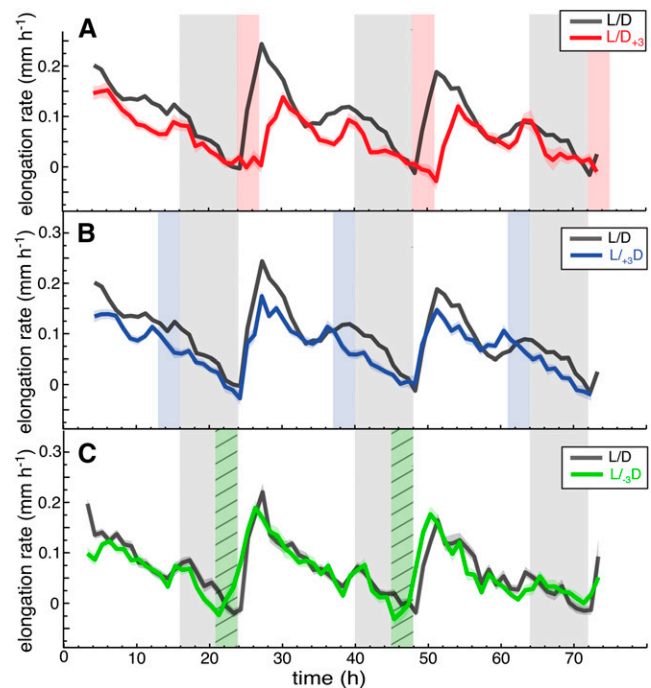
Figure 7. Light Is Required at Dawn to Trigger Leaf Growth.

(A) Leaf elongation rate of leaves 1 and 2 in long day (L/D, black line, n_{leaf} = 27) and in +3 h prolonged night period after dawn (L/D+3; red line n_{leaf} = 27).

(B) Leaf elongation rate in L/D (black line) and in +3 h prolonged night period before dusk (L/+3D; blue line, n_{leaf} = 54).

(C) Leaf elongation rate and leaf elevation angle of leaves 1 and 2 where night was shortened before dawn by −3 h (L/-3D; green line, n_{leaf} = 35; L/D control; black line, n_{leaf} = 42). Col-0 plants were grown for 14 d in standard L/D (16/8) conditions before measurement; vertical gray bars represent true night periods; vertical red/blue bars indicate prolonged night periods (**[A]** and **[B]**) and vertical hatched green bar shortened night period **(C)**. Leaf elongation rate was computed as mean moving average (3 h) of individual curves. The opaque band around the mean lines is the 95% confidence interval of mean estimate, and n_{leaf} = number of leaves. Day 1 of the experiment represents the first day when the plants were subjected to an abrupt change in night length. l_{tip} was used to compute the graphs.

we analyzed the *elf3* mutant. When grown in long days, the major growth peak of *elf3* was moved forward and was no longer dependent on light, indicating that the evening complex prevents leaf growth at night (Figure 8B, arrows) (Nozue et al., 2007). In addition, maximal growth rates in the *elf3* mutant coincided with maximal leaf angles, showing that ELF3 is needed to maintain the normal phase relationship between leaf growth and movement (Figure 8B, arrows). Analysis of *elf3* and *pif4 pif5* grown in constant light confirmed the importance of the circadian clock for rhythmic growth and movements and revealed a moderate phase phenotype in *pif4 pif5* (Figures 8C and 8D). Collectively, our data show that the mechanisms responsible for rhythmic growth in leaves and hypocotyls differ and reveal that ELF3 is required for normal phasing between leaf growth and movements.

DISCUSSION

Live measurements of leaf growth and/or leaf movements have been reported before (Wiese et al., 2007; Walter et al., 2009; Bours et al., 2012); our method is unique in that it simultaneously but separately reports on both growth and movements (Figure 3; Supplemental Figure 2). By imaging at sufficient frequency (every 10 min rather than hourly), we reduce the number of plants that we can simultaneously analyze, but this enables us to characterize circumnutations (Supplemental Figure 2C). Future work should allow us to better understand the mechanisms underlying this well-known form of "rapid" plant movements that have been discussed since the times of Charles Darwin but remain poorly understood (Whippo and Hangarter, 2009). The geometry of the laser scanning system is well suited for relatively flat and horizontally oriented objects like an *Arabidopsis* rosette. Imaging the entire leaf, in particular the blade-petiole junction, becomes difficult when leaves are erect, which is why we use l_{tip} rather than l_{leaf} (Figure 1). Importantly, our data show that l_{tip} is an excellent proxy to determine leaf elongation rates (Figure 1B). Moreover, our data correlate well with relative leaf surface growth rhythms (our own observations) and with previous publications (Wiese et al., 2007; Walter et al., 2009; Ruts et al., 2012b). However, in previous reports, in *Arabidopsis* rosettes grown in 12/12 cycles, they also identified growth peaks early in the morning and toward the end of the day similar to our data in long days (16/8; Figure 6) (Wiese et al., 2007; Ruts et al., 2012b).

By simultaneously tracking leaf movements and growth, we determined that elongation growth precedes upward movement of the leaf (Figures 3, 4, and 6, Supplemental Figures 5 and 6). This is true when analyzed at the level of the entire leaf, the blade, and the petiole (Figure 4). We thus conclude that a change in leaf hyponasty is consistent with differential petiole growth as determined before (Polko et al., 2012; Rauf et al., 2013), but in addition blade growth and elevation angle (relative to the petiole) also contribute to the overall leaf position (Figure 4). We demonstrate the importance of leaf blade position in leaf hyponasty in several growth conditions (L/L, L/D, and simulated shade), suggesting that this is a general feature of the leaf hyponastic response (Figure 4; Supplemental Figures 3 and 4). In all cases, the analyzed upward movements were initiated as the leaf (or part of it) reached its maximal elongation rate (Figures 4 and 6; Supplemental Figures 5 and 6), demonstrating a correlation between

both processes (although with temporal delays). This finding is consistent with the fact that as leaves age both growth and movements decline (Mullen et al., 2006). However, our work also reveals that coupling between growth and movements is a regulated process as environmental stimuli differentially affect growth and movements (Figure 5). For example, when PAR was diminished, the leaf growth rate declined but the leaf movements increased (Figure 5). Moreover, in the *elf3* mutant, the phase relationship between the peak of growth and elevation angle was strongly altered (Figure 8B). Growth of different parts of the blade and petiole may contribute differentially to overall growth and changes in elevation angle and thereby explain the complex relationship between growth and movement reported here (Figure 4) (Wiese et al., 2007; Andriankaja et al., 2012; Polko et al., 2012; Remmler and Rolland-Lagan, 2012). In addition, reversible turgor pressure-driven changes in cell size may also contribute to changes in leaf hyponasty (Mullen et al., 2006; Barillot et al., 2010).

By separately analyzing growth and movement of blades and petioles, we observed that blades started to grow and move upwards 2 to 3 h before the petiole (Figure 4). One possibility is that this is regulated by the combined action of auxin and carbohydrates (Lilley et al., 2012). Interestingly, rhythms in auxin responsiveness and soluble carbohydrates correlate quite well (Covington and Harmer, 2007). As the leaf blade is considered as a major source of auxin production (Tao et al., 2008), we propose that blade growth occurs before petiole growth because auxin first needs to be transported to the petiole. Interestingly, in L/L conditions, a second growth peak occurred in petioles that we did not observe in the blade (Figure 4), indicating that the growth pattern is more complex in the petiole than the blade. Based on the analysis of overall leaf growth, we can also conclude that these patterns are environmentally regulated (Figure 5). To fully understand the relationship between growth and movements, our organ-level analysis needs to be combined with the determination of growth patterns with cellular resolution, which is very challenging at the level of expanded leaves (Ichihashi et al., 2011; Andriankaja et al., 2012; Polko et al., 2012).

By moving plants into constant darkness and performing night extension or shortening experiments, we showed the requirement for light to initiate growth at dawn (Figures 6 and 7; Supplemental Figure 6B). The earlier rise of the growth rate observed in plants entrained in L/D for which the night was shortened by 3 h is consistent with the rise in growth at ZT20 observed in plants transferred into L/L (compared with Figures 3 and 7C). Importantly, when the night is extended by 3 h before the dark phase, the timing of the morning growth-peak was unaffected (Figure 7B). By contrast, extending the night by 3 h in the morning delayed the acceleration of growth until the actual onset of light (Figure 7A). Plants precisely regulate starch degradation during the night and almost completely exhaust their reserves by dawn (Stitt and Zeeman, 2012). Starch metabolism is immediately adjusted if the night is extended due to an early onset but not if the night is extended beyond the subjective dawn. Moreover, exhaustion of starch resources at the end of the night limits *Arabidopsis* growth (Graf et al., 2010). These data together with our results suggest that light at dawn fuels leaf growth if growth repression by the circadian clock is released (Figures 6 and 7; Supplemental Figure 5). Performing growth experiments in a low CO_2 environment
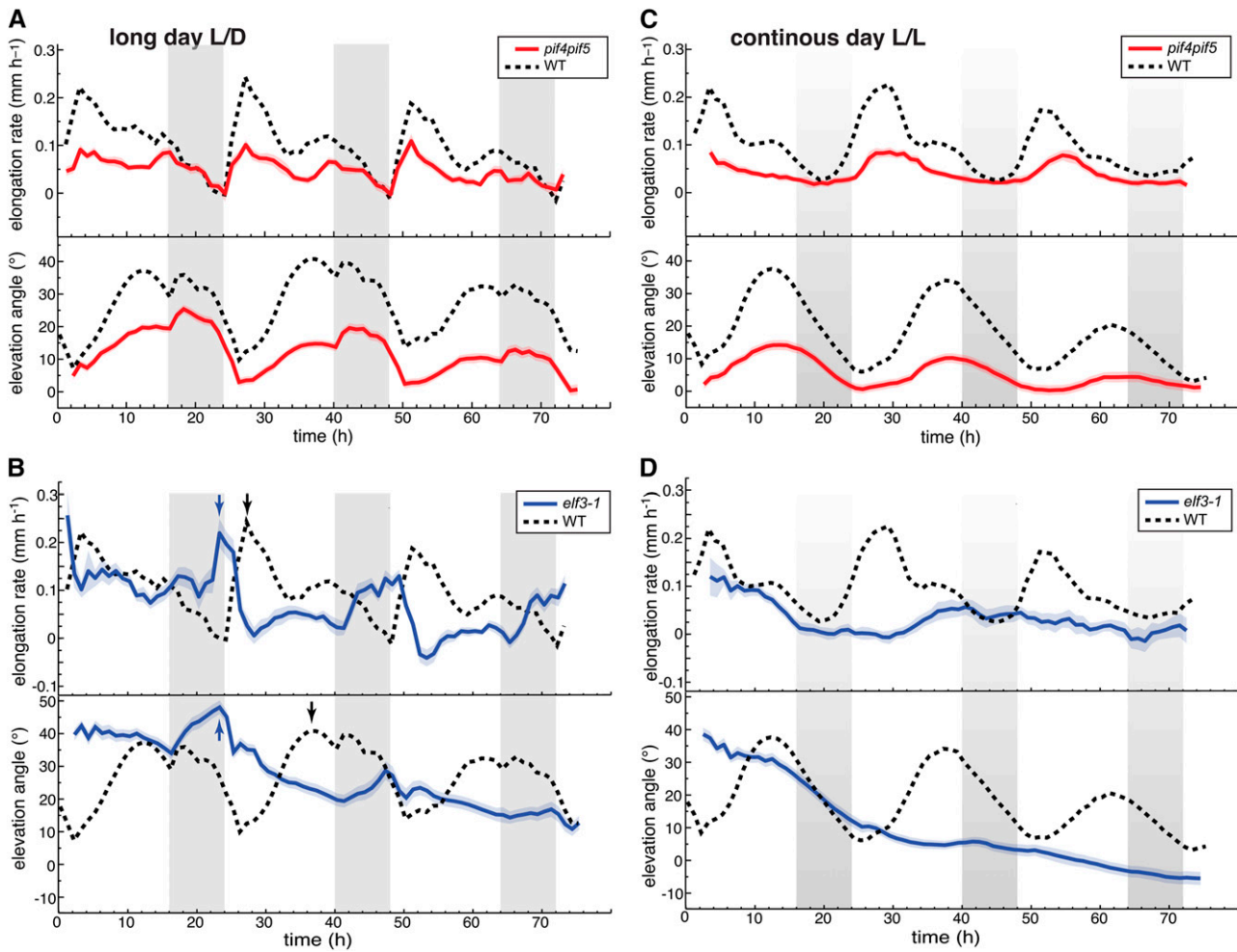
Figure 8. The Role of PIF4, PIF5, and ELF3 in Establishing Rhythmic Leaf Growth and Movement.

Leaf elongation rate and leaf elevation angle of leaves 1 and 2. Col-0, *elf3-1*, and *pif4 pif5* plants were grown for 14 d in standard L/D conditions. Beginning from time 0 h, plants were imaged either in L/D (**[A]** and **[B]**) or in L/L (**[C]** and **[D]**). Leaf elongation rate was computed as mean moving average (3 h) of individual curves. Leaf elevation angle are mean values. Vertical gray bars represent subjective or true night periods. The opaque band around the mean lines is the 95% confidence interval of mean estimate. n_{leaf} = number of measured leaves. l_{tip} and Φ_{tip} were used to compute the graphs.
(A) *pif4 pif5* double mutant grown and imaged in long-day conditions n_{leaf} = 48.
(B) Clock mutant *elf3-1* grown and imaged in long-day conditions n_{leaf} = 45. Note that in *elf3-1* the peaks of elevation angle and maximal growth coincide (blue arrows), while in the wild type there is a large phase shift between the two peaks (black arrows).
(C) *pif4 pif5* double mutant entrained in L/D and imaged in continuous light n_{leaf} = 46.
(D) *elf3-1* entrained in L/D and grown in continuous light n_{leaf} = 23.

or treating plants with photosynthesis inhibitors would be appropriate ways to further test this hypothesis. Short-day grown plants accumulate more starch during the day in order to have enough resources at night. In such conditions, fewer resources will be immediately available for growth in the morning (Stitt and Zeeman, 2012). Consistent with this idea, our data show that the morning growth peak in short-day grown plants is reduced compared with long-day-grown plants (Supplemental Figure 6A). Also consistent with this metabolic model is the relatively enhanced growth at night in short-day plants (Supplemental Figure 6A) (Sulpice et al., 2014), reduced growth in low PAR conditions (Figure 5), and the fact that

starchless mutants invest more resources in growth during the day when solar energy is present (Wiese et al., 2007). It was recently reported that a long-term consequence of sugar starvation is a reduction of gibberellin biosynthesis that limits growth (Paparelli et al., 2013). However, it is unlikely that this gibberellin response can explain the immediate effect of light on growth in the morning reported here (Figures 6 and 7). Finally, we wish to point out that when wild-type plants are kept in darkness for extended periods of time a short pulse of growth occurs ~6 to 8 h after subjective dawn (Supplemental Figure 6B). This experiment indicates that alternative metabolic pathways (e.g., induction of autophagy) can be

activated to fuel growth under exceptional circumstances (Usadel et al., 2008; Suttangkakul et al., 2011; Izumi et al., 2013).

ELF3 regulates rhythmic growth of leaves, hypocotyls, and roots (Figure 8) (Nozue et al., 2007; Nusinow et al., 2011; Yazdanbakhsh et al., 2011). Our work identifies similarities and differences for ELF3 function in these different organs. In all organs, growth at night is restricted by ELF3 (Figures 8B and 8D) (Nozue et al., 2007; Nusinow et al., 2011; Yazdanbakhsh et al., 2011). The leaf growth peak toward the end of the night in *elf3* is surprising given that in the wild type, light in the morning is essential to trigger growth (Figures 6 and 7). A possible explanation for this observation is the incomplete starch degradation during the night in *elf3* (Yazdanbakhsh et al., 2011). This may explain how this mutant has sufficient resources at the end of the night to enhance leaf growth without the need for light (Figure 8). Interestingly, long-day-grown *elf3* mutants have reduced leaf growth, contrasting with enhanced rates of root and hypocotyl growth in this mutant (Figure 8) (Nozue et al., 2007; Nusinow et al., 2011; Yazdanbakhsh et al., 2011). These organ-specific effects on growth might be due to different partitioning of resources in *elf3* (Yazdanbakhsh et al., 2011).

In hypocotyls, the circadian expression of *PIF4* and *PIF5* in conjunction with light-induced PIF4 and PIF5 protein degradation explains a rhythmic growth pattern with a major peak at dawn (Nozue et al., 2007). The analysis of leaf growth in the wild type and *pif* mutants suggests that in leaves light does not shape growth rhythms primarily by influencing PIF4 and PIF5 abundance. First, the leaf growth peak occurs several hours after dawn, which is not consistent with light-induced degradation of growth-promoting PIFs explaining this pattern (Figure 6). Second, in leaves, the *pif4 pif5* mutant maintains a growth rhythm similar to the wild type but with a reduced amplitude (Figure 8). Third, PIF4-overexpressing plants and *phyB* mutants that show reduced PIF4 degradation (de Lucas et al., 2008) maintain leaf growth rhythms with a robust amplitude in contrast to hypocotyls where this leads to dampened growth rhythms (Supplemental Figure 7) (Nozue et al., 2007). Our night extension and day-length experiments suggest that the light regulation of leaf growth has a metabolic component (Figures 6 and 7; Supplemental Figures 5 and 6). However, leaf growth patterns in constant light and reduced growth in *pif4 pif5* clearly show the importance of PIF4, PIF5, and the circadian clock in regulating this process (Figures 6 and 8; Supplemental Figure 7). Thus, rhythmic leaf and hypocotyl growth are regulated by distinct mechanisms with a different role of light in shaping growth rhythms in both organs. It will be interesting to further contrast these growth rhythms in young leaves that largely rely on their own resources with those of roots or hypocotyls that depend on photosynthates exported from the leaves.

Finally, we would like to briefly speculate on the biological significance of diel rhythms of leaf growth rates and movements. A maximal peak of growth during the first few hours of the day matches with favorable conditions in terms of energetic requirements, water availability, and auxin responsiveness (Covington and Harmer, 2007; Nozue et al., 2007; Stitt and Zeeman, 2012). Availability of resources also explains why more growth is observed at night in short-day-grown plants than in long-day-grown plants and the larger growth peak at dawn when *Arabidopsis* is grown in long days (Figure 6; Supplemental Figure 6) (Sulpice et al., 2014). The temperature cycles that accompany day-night transitions also contribute to the growth pattern (Sidaway-Lee et al., 2010; Bours et al., 2013). We note that the maximal growth rate identified in our conditions corresponds to the early morning when temperature is typically relatively low (Figure 6). Interestingly, leaf elevation follows the typical daily temperature fluctuations with a peak in the late afternoon. Elevating leaves with this pattern is favorable to cool leaves during the warm hours of the day and diminishes the radiation load at times when it surpasses photosynthetic capacity (Bridge et al., 2013).

METHODS

Plant Material and Growth Conditions

The *Arabidopsis thaliana* ecotype Columbia-0 (Col-0), the *pif4 pif5* mutant (Nozue et al., 2007), and the *elf3-1* mutant (Liu et al., 2001) were grown on soil saturated with deionized water in a Percival CU-36L4 incubator (Percival Scientific) at 21°C, $R_H = 85\%$ relative humidity, and $EP_{AR} = 180$ μmol m^{-2} s^{-1} for 13 d under long-day (16/8 h) or 17 d under short-day (8/16 h) conditions. Plants were transferred to the ScanAlyzer HTS (Lemnatec) 24 h before scanning for adaptation maintaining the day-night cycles and light conditions in the incubator. At the beginning of the scanning (at time t = 0), conditions were adjusted according to experiment (e.g., L/L or low PAR). The light intensity in the measurement chamber was $E_{PAR} = 165$ μmol m^{-2} s^{-1} and reduced to $E_{PAR} = 35$ μmol m^{-2} s^{-1} for the low PAR treatment. The red/far-red ratio (R/FR) was decreased from R/FR = 5.59 to R/FR = 0.49 using far-red-emitting diodes. Further experimental details, spectral composition of light, computation of R/FR ratio, and technical specification of the phenotyping device are described in more detail by Dornbusch et al. (2012) and are available on our website (http://plantgrowth.vital-it.ch).

Analysis of Leaf Growth Rates and Elevation Angles

Plants were scanned at intervals of 10 and 60 min. In the time-lapse images, the distance of measured plant surface points from a reference plane was color-coded (Supplemental Figure 1). Images were transformed into 3D point clouds as described by Dornbusch et al. (2012), which yields a precise representation of plant surfaces over time (Supplemental Movie 1). A detailed description of the geometric definition of leaf length and elevation angle and image and data processing is presented in the Supplemental Methods.

Supplemental Data

The following materials are available in the online version of this article.

Supplemental Figure 1. Image Analysis Algorithm to Compute P_P and P_T from Time-Lapse Images.

Supplemental Figure 2. Definition of Principal Output.

Supplemental Figure 3. In Response to a Low R/FR Treatment the Blade Upward Movement Precedes the Petiole Upward Movement.

Supplemental Figure 4. In L/D Conditions the Blade Upward Movement Precedes the Petiole upward Movement.

Supplemental Figure 5. Light Is Required at Dawn to Trigger Leaf Growth.

Supplemental Figure 6. Growth and Movements Are Altered by Shortening Daylength or in Continuous Darkness.

Supplemental Figure 7. Plants with Elevated Levels of PIF4 Maintain Leaf Growth Rhythms Robust in Amplitude.

Supplemental Methods. Detailed Description of Geometric Definition of Leaf Length and Elevation Angle, Image Processing, and Data Processing.

Supplemental Movie 1. Semiautomated Leaf Tracking on Time-Lapse 3D Images of Growing *Arabidopsis* Plant.

Supplemental Movie 2. Comparison of Leaf Tracking on 3D Images with Manual Leaf Selection on Simultaneously Photographed Growing *Arabidopsis* Plant.

AUTHOR CONTRIBUTIONS

T.D. designed research, contributed new analytic computational tools, performed research, analyzed data, and wrote the article. O.M. designed research, contributed new analytic computational tools, performed research, and analyzed data. I.X. contributed new analytic computational tools. C.F. designed research, analyzed data, and wrote the article.

REFERENCES

Andriankaja, M., Dhondt, S., De Bodt, S., Vanhaeren, H., Coppens, F., De Milde, L., Mühlenbock, P., Skirycz, A., Gonzalez, N., Beemster, G.T., and Inzé, D. (2012). Exit from proliferation during leaf development in *Arabidopsis thaliana*: a not-so-gradual process. Dev. Cell **22:** 64–78.

Barillot, R., Frak, E., Combes, D., Durand, J.L., and Escobar-Gutiérrez, A.J. (2010). What determines the complex kinetics of stomatal conductance under blueless PAR in *Festuca arundinacea*? Subsequent effects on leaf transpiration. J. Exp. Bot. **61:** 2795–2806.

Bours, R., Muthuraman, M., Bouwmeester, H., and van der Krol, A. (2012). OSCILLATOR: A system for analysis of diurnal leaf growth using infrared photography combined with wavelet transformation. Plant Methods **8:** 29.

Bours, R., van Zanten, M., Pierik, R., Bouwmeester, H., and van der Krol, A. (2013). Antiphase light and temperature cycles affect PHYTOCHROME B-controlled ethylene sensitivity and biosynthesis, limiting leaf movement and growth of Arabidopsis. Plant Physiol. **163:** 882–895.

Bridge, L.J., Franklin, K.A., and Homer, M.E. (2013). Impact of plant shoot architecture on leaf cooling: a coupled heat and mass transfer model. J. R. Soc. Interface **10:** 20130326.

Covington, M.F., and Harmer, S.L. (2007). The circadian clock regulates auxin signaling and responses in Arabidopsis. PLoS Biol. **5:** e222.

de Lucas, M., Davière, J.M., Rodríguez-Falcón, M., Pontin, M., Iglesias-Pedraz, J.M., Lorrain, S., Fankhauser, C., Blázquez, M.A., Titarenko, E., and Prat, S. (2008). A molecular framework for light and gibberellin control of cell elongation. Nature **451:** 480–484.

Dornbusch, T., Lorrain, S., Kuznetsov, D., Fortier, A., Liechti, R., Xenarios, I., and Fankhauser, C. (2012). Measuring the diurnal pattern of leaf hyponasty and growth in Arabidopsis - a novel phenotyping approach using laser scanning. Funct. Plant Biol. **39:** 860–869.

Farré, E.M. (2012). The regulation of plant growth by the circadian clock. Plant Biol. (Stuttg.) **14:** 401–410.

Graf, A., Schlereth, A., Stitt, M., and Smith, A.M. (2010). Circadian control of carbohydrate availability for growth in Arabidopsis plants at night. Proc. Natl. Acad. Sci. USA **107:** 9458–9463.

Ichihashi, Y., Kawade, K., Usami, T., Horiguchi, G., Takahashi, T., and Tsukaya, H. (2011). Key proliferative activity in the junction between the leaf blade and leaf petiole of Arabidopsis. Plant Physiol. **157:** 1151–1162.

Izumi, M., Hidema, J., Makino, A., and Ishida, H. (2013). Autophagy contributes to nighttime energy availability for growth in Arabidopsis. Plant Physiol. **161:** 1682–1693.

Keller, M.M., Jaillais, Y., Pedmale, U.V., Moreno, J.E., Chory, J., and Ballaré, C.L. (2011). Cryptochrome 1 and phytochrome B control shade-avoidance responses in Arabidopsis via partially independent hormonal cascades. Plant J. **67:** 195–207.

Lilley, J.L.S., Gee, C.W., Sairanen, I., Ljung, K., and Nemhauser, J.L. (2012). An endogenous carbon-sensing pathway triggers increased auxin flux and hypocotyl elongation. Plant Physiol. **160:** 2261–2270.

Liu, X.L., Covington, M.F., Fankhauser, C., Chory, J., and Wagner, D.R. (2001). ELF3 encodes a circadian clock-regulated nuclear protein that functions in an Arabidopsis PHYB signal transduction pathway. Plant Cell **13:** 1293–1304.

Moreno, J.E., Tao, Y., Chory, J., and Ballaré, C.L. (2009). Ecological modulation of plant defense via phytochrome control of jasmonate sensitivity. Proc. Natl. Acad. Sci. USA **106:** 4935–4940.

Mullen, J.L., Weinig, C., and Hangarter, R.P. (2006). Shade avoidance and the regulation of leaf inclination in Arabidopsis. Plant Cell Environ. **29:** 1099–1106.

Nozue, K., Covington, M.F., Duek, P.D., Lorrain, S., Fankhauser, C., Harmer, S.L., and Maloof, J.N. (2007). Rhythmic growth explained by coincidence between internal and external cues. Nature **448:** 358–361.

Nusinow, D.A., Helfer, A., Hamilton, E.E., King, J.J., Imaizumi, T., Schultz, T.F., Farré, E.M., and Kay, S.A. (2011). The ELF4-ELF3-LUX complex links the circadian clock to diurnal control of hypocotyl growth. Nature **475:** 398–402.

Paparelli, E., Parlanti, S., Gonzali, S., Novi, G., Mariotti, L., Ceccarelli, N., van Dongen, J.T., Kölling, K., Zeeman, S.C., and Perata, P. (2013). Nighttime sugar starvation orchestrates gibberellin biosynthesis and plant growth in Arabidopsis. Plant Cell **25:** 3760–3769.

Polko, J.K., van Zanten, M., van Rooij, J.A., Marée, A.F., Voesenek, L.A., Peeters, A.J., and Pierik, R. (2012). Ethylene-induced differential petiole growth in *Arabidopsis thaliana* involves local microtubule reorientation and cell expansion. New Phytol. **193:** 339–348.

Rauf, M., Arif, M., Fisahn, J., Xue, G.P., Balazadeh, S., and Mueller-Roeber, B. (2013). NAC transcription factor speedy hyponastic growth regulates flooding-induced leaf movement in Arabidopsis. Plant Cell **25:** 4941–4955.

Remmler, L., and Rolland-Lagan, A.G. (2012). Computational method for quantifying growth patterns at the adaxial leaf surface in three dimensions. Plant Physiol. **159:** 27–39.

Ruts, T., Matsubara, S., Wiese-Klinkenberg, A., and Walter, A. (2012a). Diel patterns of leaf and root growth: endogenous rhythmicity or environmental response? J. Exp. Bot. **63:** 3339–3351.

Ruts, T., Matsubara, S., Wiese-Klinkenberg, A., and Walter, A. (2012b). Aberrant temporal growth pattern and morphology of root

and shoot caused by a defective circadian clock in *Arabidopsis thaliana*. Plant J. **72:** 154–161.

Sidaway-Lee, K., Josse, E.M., Brown, A., Gan, Y., Halliday, K.J., Graham, I.A., and Penfield, S. (2010). SPATULA links daytime temperature and plant growth rate. Curr. Biol. **20:** 1493–1497.

Stewart, J.L., Maloof, J.N., and Nemhauser, J.L. (2011). PIF genes mediate the effect of sucrose on seedling growth dynamics. PLoS ONE **6:** e19894.

Stitt, M., and Zeeman, S.C. (2012). Starch turnover: pathways, regulation and role in growth. Curr. Opin. Plant Biol. **15:** 282–292.

Stolarz, M. (2009). Circumnutation as a visible plant action and reaction: physiological, cellular and molecular basis for circumnutations. Plant Signal. Behav. **4:** 380–387.

Sulpice, R., Flis, A., Ivakov, A.A., Apelt, F., Krohn, N., Encke, B., Abel, C., Feil, R., Lunn, J.E., and Stitt, M. (2014). Arabidopsis coordinates the diurnal regulation of carbon allocation and growth across a wide range of photoperiods. Mol. Plant **7:** 137–155.

Suttangkakul, A., Li, F., Chung, T., and Vierstra, R.D. (2011). The ATG1/ATG13 protein kinase complex is both a regulator and a target of autophagic recycling in Arabidopsis. Plant Cell **23:** 3761–3779.

Tao, Y., et al. (2008). Rapid synthesis of auxin via a new tryptophan-dependent pathway is required for shade avoidance in plants. Cell **133:** 164–176.

Usadel, B., Bläsing, O.E., Gibon, Y., Retzlaff, K., Höhne, M., Günther, M., and Stitt, M. (2008). Global transcript levels respond to small changes of the carbon status during progressive exhaustion of carbohydrates in Arabidopsis rosettes. Plant Physiol. **146:** 1834–1861.

Walter, A., Silk, W.K., and Schurr, U. (2009). Environmental effects on spatial and temporal patterns of leaf and root growth. Annu. Rev. Plant Biol. **60:** 279–304.

Whippo, C.W., and Hangarter, R.P. (2009). The "sensational" power of movement in plants: A Darwinian system for studying the evolution of behavior. Am. J. Bot. **96:** 2115–2127.

Wiese, A., Christ, M.M., Virnich, O., Schurr, U., and Walter, A. (2007). Spatio-temporal leaf growth patterns of Arabidopsis thaliana and evidence for sugar control of the diel leaf growth cycle. New Phytol. **174:** 752–761.

Yazdanbakhsh, N., Sulpice, R., Graf, A., Stitt, M., and Fisahn, J. (2011). Circadian control of root elongation and C partitioning in *Arabidopsis thaliana*. Plant Cell Environ. **34:** 877–894.